Supplementary Materials for

Somites Without a Clock

Ana S. Dias, Irene de Almeida, Julio M. Belmonte, James A. Glazier, Claudio D. Stern*

*Corresponding author. E-mail: c.stern@ucl.ac.uk

Published 9 January 2014 on *Science* Express
DOI: 10.1126/science.1247575

This PDF file includes:

Other Supplementary Material for this manuscript includes the following:
(available at www.sciencemag.org/cgi/content/full/science.1247575/DC1)

Materials and Methods

Grafting and other techniques are essentially the same as previously described (1-4) except for Noggin treatments. Donor embryos were either quail embryos (obtained from B C Potter, Farm, UK) or a transgenic line of chick embryos expressing GFP ubiquitously (5). Host embryos were Brown Bovan Gold (obtained from Henry Stewart & Co., UK). The most posterior 1/3 or so of the primitive streak was excised from the donor embryo at stage-5 (6) (or as indicated) and placed into a drop of Noggin protein solution at 1.5 µg/ml in PBS containing 0.1% BSA for 3 hours (see Table S1 for calibration of Noggin concentration). The explant was then placed in the anterior-lateral extraembryonic area opaca of a host embryo at stage-5 and surrounded by 5-8 heparin-acrylic beads (Sigma) soaked in the same Noggin solution. The embryo was cultured by a modification of New's method (7) for the required time before fixing and processing for antibody staining and in situ hybridization by usual procedures. The host embryo was unaffected by the presence of Noggin beads in the extraembryonic area, as described in previous studies (1, 8).

To analyze the longer term fate of the ectopic somites, a single somite was dissected from those formed from the explant with light Trypsin (Difco 1:250; 0.12% w/v in Tyrode's saline). A single somite from the lower cervical/upper thoracic region of a host embryo at stage 11-12 was removed using a surgical micro-knife in ovo, in the presence of trypsin (as above). The trypsin solution was rinsed off with Tyrode's and the ectopic somite grafted in place of the excised one. The egg was sealed and the operated embryo incubated for 2-4 days up to stage 22-25.

Antibodies used were directed to chick Fibronectin (VA1(3)-S), N-cadherin, neurofilament-associated protein (3A10) and the HNK-1 epitope (IC10). All were obtained from the Developmental Studies Hybridoma Bank, Iowa, USA apart from the anti-N-cadherin antibody which was a rat monoclonal antibody obtained from InVitrogen. Grafted embryos (stained as whole mounts with IC10, 3A10, or by in situ hybridization for Pax1 or MyoD) were sectioned in a vibratome at 50µm and then stained with rabbit anti-GFP antibody (InVitrogen). Partial Dapper1 and Dapper2 cDNA probes were kindly provided by Dr. S. Dietrich (9); we subsequently isolated a 1.1kb cDNA encoding chick Dapper1. Somite sizes were measured in whole embryos using a 10x objective and from Z-stacks of multi-photon confocal sections through embryos double-immunostained for Fibronectin and N-cadherin, using Image-J software. Time-lapse video filming was performed by conventional fluorescence microscopy using an Olympus inverted microscope and Simple PCI software.

Supplementary Text

Formation of ectopic somites may occur without passing through a presomitic mesoderm-like state.

To test whether formation of ectopic somites is preceded by a presomitic-mesoderm-like state, we used the presomitic and somite markers *Dapper1* and *Dapper2* (*9*) in mesoderm explants in time-course. None of the primitive streak explants showed expression of the somite marker *Dapper2* prior to somite formation at 6 (0/10) or 8 (0/5) hours, while all explants expressed the presomitic marker *Dapper1* (6/6) and none

expressed *Dapper2* (0/6) at 11 hours when somites were present. However it is less clear whether somite formation is preceded by a presomitic-mesoderm-like state: only 1/17 explants expressed *Dapper1* after 6 hours and 2/17 after 8 hours (see Fig. S4). These observations suggest that Noggin-treated mesoderm may be able to generate somites without passing through a typical presomitic mesoderm-like state.

Computational methods

Glazier-Graner-Hogeweg (*GGH*) computational model

The GGH computational model represents space as a regular cell lattice of sites (Fig. S5), each containing an integer *index*. A GGH *generalized cell* may represent a biological cell, a subcompartment or region of a cell, or a portion of non-cellular material or fluid medium. Each generalized cell is an extended domain of sites that share a common index (σ) (Fig. S5, right). The cell-lattice configuration corresponds to an *effective energy* (H), defined so that simulated **cells** have the desired properties, behaviors and interactions, implemented via constraint terms in H. In our model **cells** have volumes, and interact via adhesion and dynamical cell-cell pulling forces, so that H has the following form:

$$H = \sum_{\substack{\vec{i}\,\vec{j} \\ \text{neighbors}}} J\left(\tau\left(\sigma_{\vec{i}}\right), \tau\left(\sigma_{\vec{j}}\right)\right) \cdot \left(1 - \delta\left(\sigma_{\vec{i}}, \sigma_{\vec{j}}\right)\right) + \sum_{\sigma} \lambda_{\text{vol}}(\sigma) \cdot \left(v(\sigma) - V_{\text{t}}(\sigma)\right)^2 + \sum_{\sigma,\sigma'} \lambda_{\text{F}} \cdot \left(l(\sigma,\sigma') - L_{\text{t}}\right)^2$$

(Equation 1)

The first sum, over all pairs of neighboring lattice sites $\vec{i}$ and $\vec{j}$, calculates the *boundary* or *contact energy* between neighboring **cells**, $\sigma_{\vec{i}}$ and $\sigma_{\vec{j}}$. $J\left(\tau\left(\sigma_{\vec{i}}\right), \tau\left(\sigma_{\vec{j}}\right)\right)$ is the boundary energy per unit contact area for **cells** of types $\tau\left(\sigma_{\vec{i}}\right)$ and $\tau\left(\sigma_{\vec{j}}\right)$ occupying sites $\vec{i}$ and $\vec{j}$, respectively, and the delta function restricts the contact energy contribution to **cell-cell** interfaces (sites belonging to the same generalized cell have zero contact energy).

The second sum in (Eq. 1) over all **cells**, calculates the effective energies due to the volume constraint. Deviations of the volume of **cell** $v(\sigma)$ from its target value $V_{\text{t}}(\sigma)$ increase the effective energy, penalizing these deviations. On average, a **cell** will occupy a number of sites in the cell lattice slightly smaller than its target volume due to surface tensions from the contact energies (J). The parameter λ_{vol} behave like Young's moduli, with higher values reducing fluctuations of a **cell**'s volume about its target value.

The third sum in (Eq. 1) represents a spring force between the center of mass of each connected cell as described later.

Cell dynamics in the GGH model provide a much simplified representation of cytoskeletally-driven cell motility using a stochastic modified Metropolis algorithm consisting of a series of index-copy attempts: the algorithm randomly selects a target site $\vec{i}$ and a neighboring source site $\vec{i}'$; if different **cells** occupy those sites the algorithm sets $\sigma_{\vec{i}} = \sigma_{\vec{i}'}$ with a probability given by the Boltzmann acceptance function:

$$P\left(\sigma_{\vec{i}} \rightarrow \sigma_{\vec{i}'}\right) = \begin{cases} 1 & : \quad \Delta H \leq 0 \\ e^{-\frac{\Delta H}{T_m}} & : \quad \Delta H > 0 \end{cases},$$

(Equation 2)

where ΔH is the change in the effective energy if the copy occurs and T_m is a global parameter describing the amplitude of **cell** membrane fluctuations. A Monte Carlo Step (*MCS*) is defined as *N* index-copy attempts, where *N* is the number of sites in the cell lattice, and sets the natural unit of time in the simulation. The Metropolis algorithm evolves the cell-lattice configuration to simultaneously satisfy the constraints, to the extent to which they are compatible, with perfect damping (*i.e.*, average velocities are proportional to applied forces).

For a further introduction to GGH modeling, see Swat *et al.* (*10*).

Simulation dynamics

The simulations represent a two-dimensional section through a three-dimensional tissue. Initially all cells are of type **Mesenchymal** and are distributed in a rectangle as an isotropic aggregate. An external fluid **Medium** surrounds the aggregate and **Epithelial** cells secrete a fluid extracellular material **ECM** that will later form the **Lumen** at the center of the somites (Fig. S6 A). After a transition period to relax the artificial initial pattern, we mimic the addition of Noggin in vitro, by changing all **Mesenchymal** cells to **Epithelial** cells (Fig. S6 B).

Epithelial cell contain 3 internal compartments: **Apical** (green cells in Fig. S5), **Lateral** (blue) and **Basal** (red). These 3 compartments are initially distributed randomly inside the **Epithelial** cell and later reorganize. Based on N-cadherin staining experiments (*11*), we assume very strong adhesion between **Apical** compartments.

Linear elastic spring links connect the internal compartments of each **Epithelial** cell and drive the cell's elongation (Fig. S5, bottom-right). The third sum in Equation 1, implements these forces, where l is the actual distance between the two compartments, L_t is the target distance between them, and λ_F is the spring constant. The spring constant of the links remains constant, while the target distance between the compartments is initially low and increases at a constant rate during the simulation, elongating the polarized cells.

The **Basal** compartments of the **Epithelial** cells secretes **ECM** (dark red, Fig. S5, left). The **ECM** adheres strongly to **Medium** and to the **Basal** compartments of **Epithelial** cells. It forms a thin layer between the somites and helps to stabilize their shape. **Basal** compartments stop secreting **ECM** once they cease to contact other **Epithelial** cells or **Medium**.

As the **Epithelial** cells rearrange, the **ECM** between the cells becomes trapped inside the forming somites and forms a **Lumen**. Neighboring **Apical** compartments in adjacent **Epithelial** cells that touch the same **Lumen** and stay in contact with each other for an extended period of time develop apical junctions between them, which we represent by creating elastic springs between the neighboring **Apical** compartments.

We also implement two polarity induction mechanisms from Martins *et al.* (*11*). If an **Epithelial** cell's **Apical** compartment fails to contact other **Apical** compartments

and/or **Lumen**, it forms a transient elastic link with the nearest **Apical** compartment. The same happens for **Basal** compartments. In addition, **Epithelial** cells can reverse their elongation temporally if they find themselves in an odd position with respect to the surrounding cells. Polarity induction accelerates somite formation and prevents the formation of small orphaned clusters of cells.

Fig. S1.

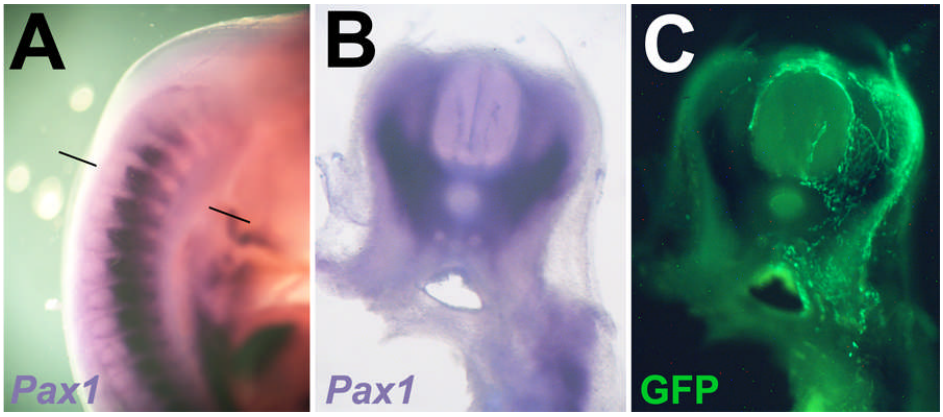

Embryo transplanted with an ectopic somite in the cervical region at stage 10 as shown in Fig. 1L, then incubated to stage 25 and processed by in situ hybridization for expression of the sclerotomal marker *Pax1*. A. The somite has integrated well and expresses *Pax1* indistinguishably from the host. B is a transverse section through the ectopic somite at the level indicated by the dashes in A, and C reveals the GFP expression after staining the same section with anti-GFP antibody and an Alexa-488 labeled second antibody to reveal the cells derived from the transplanted somite.

Fig. S2

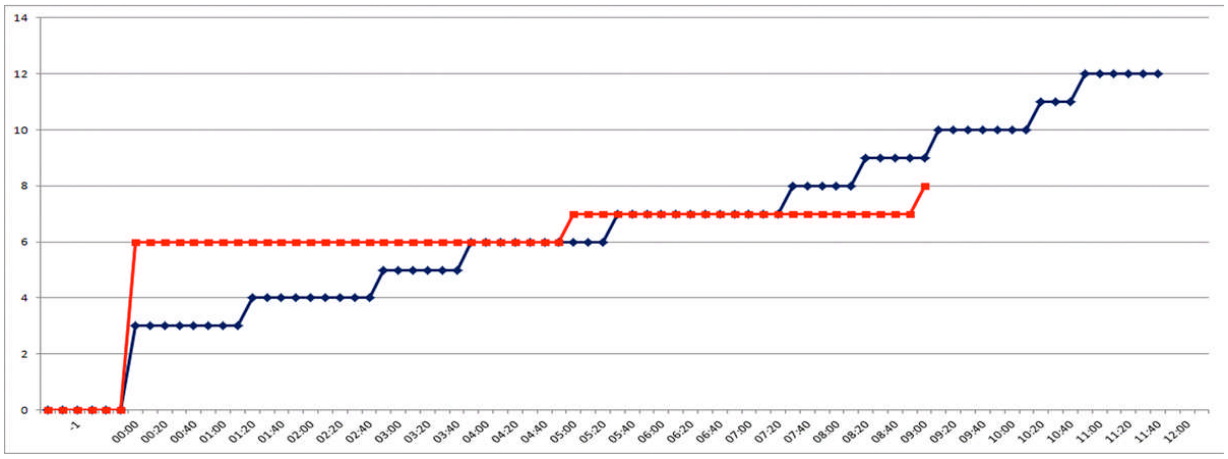

The ectopic somites in the explants form almost simultaneously; this graph compares the number of somites formed at 10 min intervals in a control embryo (blue) and a graft (red), measured from time-lapse films like those in Movies S1-S3. The formation of the first somite to appear is taken as t=0:00. The plot begins at 1 hour before this (t= -1:00 h). In this case, 6 somites form simultaneously from the graft.

Fig. S3

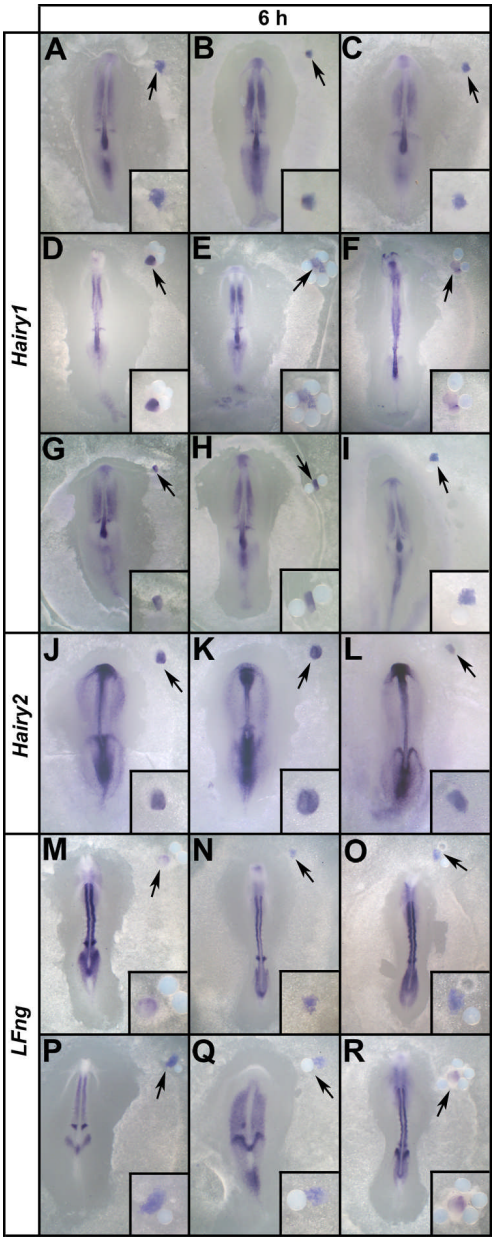

No evidence of molecular oscillations of “clock genes” in explants. This figure relates to Fig. 2 which showed no variation for *Hairy1*, *Hairy2* or *LFng* at different time points after Noggin treatment of the explant. Here, many embryos are shown for a single time point, 6 hours after grafting into the host. A-I are 9 examples for *Hairy1*, J-L are examples for *Hairy2* and M-R are examples for *LFng*. For all three genes, note the typical variation of patterns of expression in the presomitic mesoderm of the host embryo, revealing the host “segmentation clock”, and the comparative invariance of expression in the explants (arrows and insets).

Fig. S4

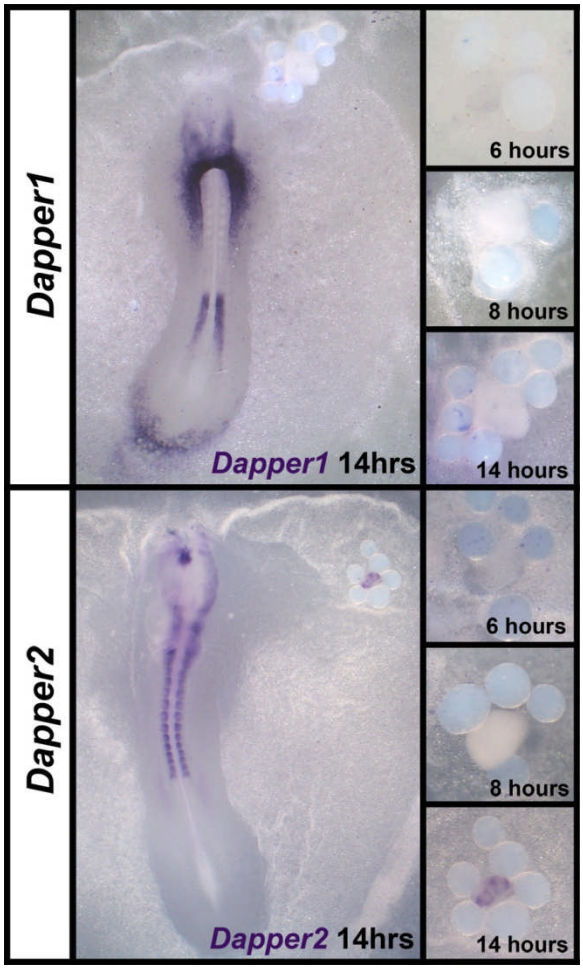

Formation of ectopic somites does not appear to be preceded by a pre-somitic mesoderm-like state. We used *Dapper1* as marker of presomitic mesoderm and *Dapper2* as marker of formed somites (the normal patterns of expression are seen in the host embryo in the large panel on the left). Explants are shown harvested at 6, 8 and 14 hours. Neither gene is expressed before somites form. When somites appear, they express *Dapper2* only (lower right panel, 14 hour time point).

Fig. S5

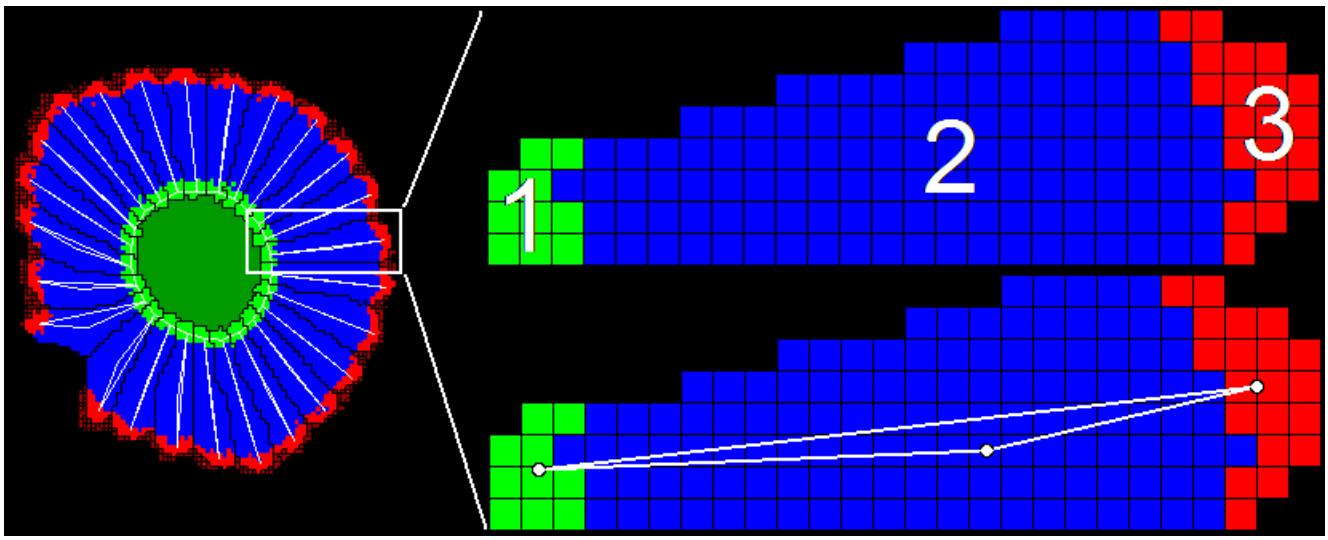

Implementation of epithelial cells in an ectopic somite in the GGH model. Each cell is a collection of cell lattice sites that share a common cell index but differing compartment indices. Colors represent compartments of the same type and share the same parameter values. The upper right shows a close-up of an **Epithelial** cell with its 3 compartments. The bottom right panel shows the elastic links in white connecting the compartments within a cell that drive and maintain cell elongation. Dark green, **Lumen**; dark red, **ECM**; green, **Apical** compartments; blue **Lateral** compartments; red **Basal** compartments.

Fig. S6

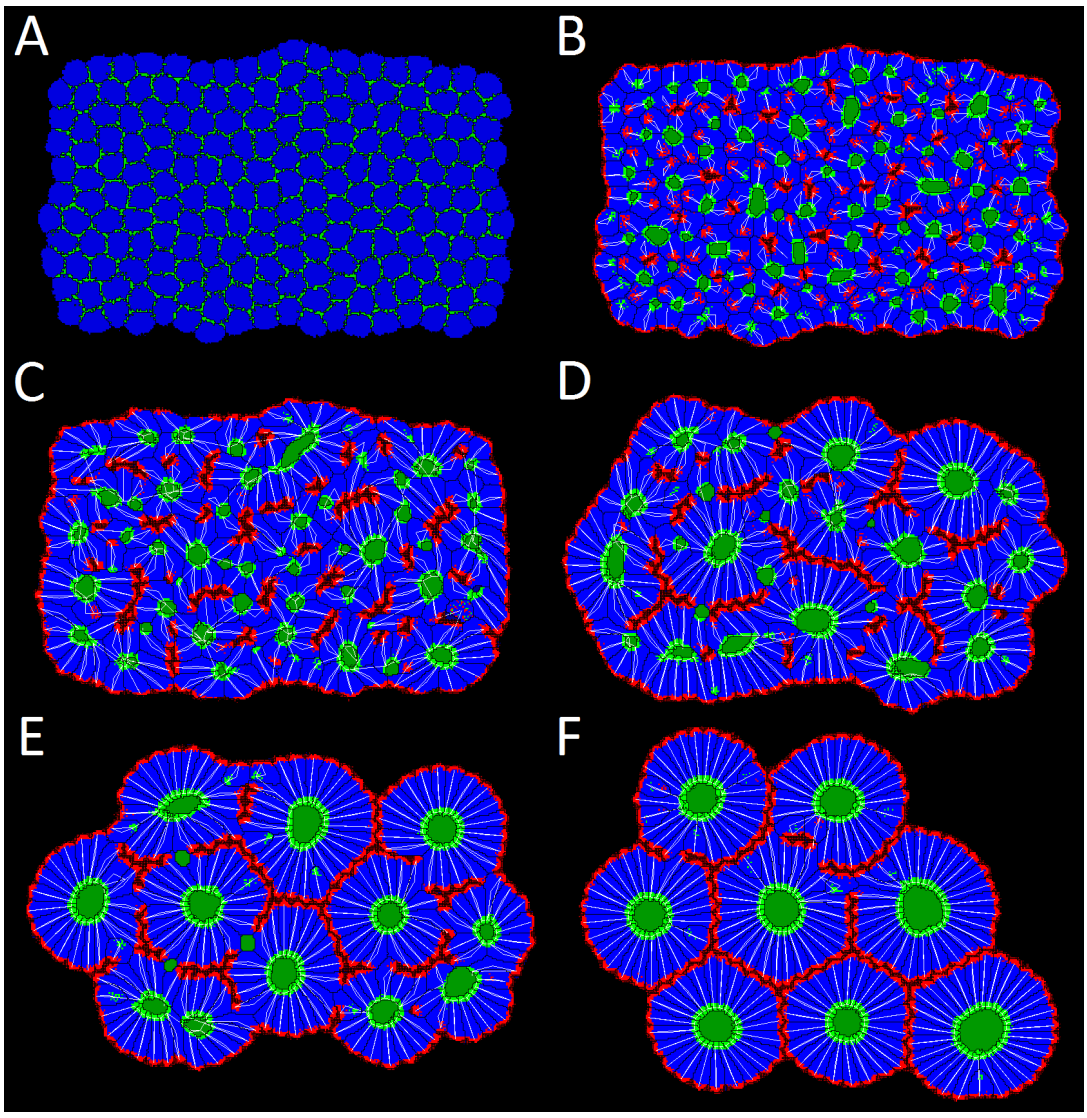

Typical time course of ectopic somite simulation. (**A**) Initially all cells are **Mesenchyme** and distributed in a roughly rectangular domain surrounded by **Medium**. (**B**) After exposure to Noggin, all cells become **Epithelial** MET, increase their adhesion to each other. (**C**) The polarized **Epithelial** cells start to elongate and secrete **ECM**. (**B**-**E**) As cells rearrange, the internal liquid is displaced and accumulates at the center of the forming ectopic somites. (**F**) The cells eventually stabilize and form ectopic somites of roughly uniform shape and size. Snapshots at 4000, 5000, 6000, 10000, 20000 and 500000 MCS.

Table S1.

Effects of Noggin concentration on the number of ectopic somites formed

2.5µg/ml Noggin			**% embryos with ectopic somites**		
Hpg	Total *n*	Embryos w/ectopic somites	Total	Bunch of grapes	In a line
5	30	0	0	0	0
9	90	60	67%	17%	83%
12	75	33	44%	39%	61%
15	68	38	56%	53%	47%

1.5µg/ml Noggin			**% embryos with ectopic somites**		
Hpg	Total *n*	Embryos w/ectopic somites	Total	Bunch of grapes	In a line
5	10	0	0	0	0
9	30	20	66%	72%	28%
12	25	12	50%	75%	25%
15	16	10	63%	81%	19%

Hpg, hours post-graft

Movie S1

Formation of ectopic somites generated from a graft of stage 5 posterior primitive streak from a transgenic-GFP donor embryo, soaked in Noggin and then grafted into the area opaca of a wild-type host chick embryo, surrounded by beads soaked in Noggin. Many ectopic somites form almost simultaneously around 10-11 hours after grafting.

Movie S2

Higher magnification view of the region of the graft (fluorescence channel only) from Supplementary Movie 1, showing almost simultaneous formation of ectopic somites.

Movie S3

Formation of somites in a normal embryo. Embryo placed in modified New culture at stage 4 and incubated for about 24 hours. At about 8.5 hours (stage 6-8), the first 3 pairs of occipital somites form almost simultaneously. Thereafter somites form sequentially, about one pair every 90 min.

Movie S4

Simulation of ectopic somite formation using CompuCell3D as described in Computational Methods.

References cited in Supplementary Information

1. A. Streit, C. D. Stern, Mesoderm patterning and somite formation during node regression: differential effects of chordin and noggin. *Mech Dev* **85**, 85 (1999).
2. C. D. Stern, in *Essential Developmental Biology: A Practical Approach*, C. D. Stern, P. W. H. Holland, Eds. (IRL Press/Oxford University Press, Oxford, 1993), pp. 45-54.
3. C. D. Stern, Grafting of somites. *Methods Mol Biol* **97**, 255 (1999).
4. A. Streit, C. D. Stern, Operations on primitive streak stage avian embryos. *Methods Cell Biol* **87**, 3 (2008).
5. H. Sang, Prospects for transgenesis in the chick. *Mech Dev* **121**, 1179 (2004).
6. V. Hamburger, H. L. Hamilton, A series of normal stages in the development of the chick embryo. *J Morphol* **88**, 49 (1951).
7. C. D. Stern, G. W. Ireland, An integrated experimental study of endoderm formation in avian embryos. *Anat Embryol* **163**, 245 (1981).
8. A. Tonegawa, N. Funayama, N. Ueno, Y. Takahashi, Mesodermal subdivision along the mediolateral axis in chicken controlled by different concentrations of BMP-4. *Development* **124**, 1975 (1997).
9. L. E. Alvares *et al.*, Chicken dapper genes are versatile markers for mesodermal tissues, embryonic muscle stem cells, neural crest cells, and neurogenic placodes. *Dev Dyn* **238**, 1166 (2009).
10. M. H. Swat *et al.*, Multi-Scale Modeling of Tissues Using CompuCell3D. *Method Cell Biol* **110**, 325 (2012).
11. G. G. Martins *et al.*, Dynamic 3D cell rearrangements guided by a fibronectin matrix underlie somitogenesis. *PLoS One* **4**, e7429 (2009).